Cellular Signalling 54 (2019) 150–160

Contents lists available at ScienceDirect

Cellular Signalling

journal homepage: www.elsevier.com/locate/cellsig

miRNA networks modulate human endothelial cell adaptation to cyclic hypoxia

Kinga Kochan-Jamrozy[a], Jarosław Króliczewski[a], Adrianna Moszyńska[a], James F. Collawn[b], Rafal Bartoszewski[a,*]

[a] Department of Biology and Pharmaceutical Botany, Medical University of Gdansk, Gdansk, Poland
[b] Department of Cell, Developmental and Integrative Biology, University of Alabama at Birmingham, Birmingham, USA

ARTICLE INFO

Keywords:
microRNA
HUVEC
Cyclic hypoxia
Angiogenesis
miR-19a-5p
Endothelin B receptor

ABSTRACT

Solid tumor microenvironments are often subjected to various levels of hypoxia. Although regulation of gene expression has been examined extensively, most studies have focused on prolonged hypoxia. The tumor microenvironment, however, experiences waves of hypoxia and reoxygenation that stimulate the expression of pro-angiogenic factors that promote blood vessel formation. In this study, we examined human umbilical vascular endothelial cells (HUVECs) under waves of intermittent (cyclic) hypoxia to determine how this process compares to prolonged hypoxia, and more importantly, how this influences the microRNA profiles that potentially affect the posttranscriptional regulation of angiogenic genes. The rationale for these studies is that cancer cells subjected to cyclic hypoxia appear to have increased metastatic potential and endothelial cells exhibit a higher radiation resistance and greater migration potential. This indicates that gene regulatory networks in cyclic hypoxia may be different from prolonged hypoxia. Here we examined the consequences of cyclic hypoxia on miRNA gene expression and how these changes in miRNA expression influence angiogenesis. Using Next Generation Sequencing, our results demonstrate that cyclic hypoxia has very different effects on the miRNA networks compared to prolonged hypoxia, and that the *in silico* predicted effects on the certain mRNA target genes are more similar than might be expected. More importantly, these studies indicate that identifying potential miRNAs (including hsa-miR-19a-5p) as therapeutic targets for inhibiting angiogenesis and tumor progression will require this type of physiologically relevant analysis.

1. Introduction

Hypoxia, as a feature of almost all solid tumor microenvironments, often contributes to a tumor's aggressive phenotype and therapy resistance [1]. Cyclic hypoxia affects tumor growth and results in increased vascularization of growing tumors during periods of alternating states of low oxygen concentration and reoxygenation. This process has been defined previously as intermittent or acute hypoxia [2]. Two general frequency patterns of fluctuating changes have been observed in tumor microenvironments. Low frequency changes often result from blood vessel creation or remodeling processes that can last hours or even days. High frequency fluctuations can last from minutes to hours and are caused by a decreased erythrocyte flux or a temporary lack of blood flow [3,4].

Hypoxic conditions affect not only malignant tissues, but also the blood vessels that nurture the tumor [2,3,5]. Although tumors express various pro-angiogenic factors that stimulate angiogenesis, the resulting vessels are often disorganized and structurally and functionally abnormal [6]. This aberrant tumor vasculature and tumor compression by proliferating cancer cells result in irregular blood flow and contribute to cyclic hypoxia [7,8]. Furthermore, since the cyclic hypoxia affects both cancer and endothelial cells, it is important that an effective adaptation of the endothelium to low oxygen levels is required for survival and tumor development [5].

Between the two types of hypoxia, prolonged hypoxia is well characterized, whereas cyclic hypoxia appears to be more resistant to cancer therapy. Cancer cells subjected to repeating cycles of hypoxia and reoxygenation demonstrate increased metastatic potential, and endothelial cells exhibit a higher radiation resistance, and a greater migration potential and tube formation ability [8–11]. This suggests a number of implications for tumor cell survival, delivery and responsiveness to chemotherapeutic agents and tumor regrowth potential. Furthermore, these observations have been demonstrated in different whole genome expression profiles of both cancer and endothelial tissues

* Corresponding author at: Department of Biology and Pharmaceutical Botany, Medical University of Gdansk, Hallera 107, 80-416 Gdansk, Poland.
E-mail address: rafalbar@gumed.edu.pl (R. Bartoszewski).

https://doi.org/10.1016/j.cellsig.2018.11.020
Received 7 September 2018; Received in revised form 24 November 2018; Accepted 26 November 2018
Available online 12 December 2018

under cyclic and prolonged hypoxia conditions [3,12].

Although numerous studies have proposed that cyclic hypoxia is a critical target for tumor response therapies, the molecular mechanisms involved in cyclic hypoxia responses remain poorly understood. Furthermore, most of the previous studies have focused on the hypoxic microenvironment in tumor cells, while the consequences of cyclic hypoxia on tumor blood vessel formation have been overlooked [13]. Although the role of miRNAs in the molecular responses to low oxygen levels has been extensively studied [14,15], the specific role of miRNAs in cyclic hypoxia remains limited despite their potentially far-reaching implications in many forms of cancer. Importantly, the function of miRNAs in human endothelial cells during cyclic hypoxia has not been investigated. Given the potential role of miRNAs during cyclic hypoxia in regulating angiogenesis and cell survival, these RNAs could potentially play an important role in inhibiting tumor progression.

In the present studies using Next Generation Sequencing, we followed the specific alterations in the miRNA levels during cyclic hypoxia in primary human umbilical vein endothelial cells (HUVECs). The results of these experiments illustrate that cyclic hypoxia is very different than prolonged hypoxia and has a very different effect on miRNA profiles in endothelial cells. Our *in silico* analysis, however, suggests that the changes in miRNA networks induced by cyclic hypoxia modulate the same signaling pathways that are responsible for the response to prolonged hypoxia. Furthermore, we demonstrate that miR-19a-5p is specifically reduced during cyclic hypoxia, and we discuss how this could be a potential therapeutic target.

2. Results

The goal of this study was to test whether cyclic hypoxia has specific effects on the miRNA profiles in human endothelial cells (ECs), and more specifically with miRNAs involved in angiogenesis and cell survival. To address this, we utilized Next Generation Sequencing (NGS) to follow changes in miRNA levels in primary HUVECs exposed to cyclic and prolonged hypoxia.

Cyclic hypoxia inside vascularized tumors is defined as a recurrent phenomenon that is composed of relatively short periods of alternating hypoxia and reoxygenation. In this study, we applied parameters of hypoxia/reoxygenation cycling that are widely established in literature [8,16,17]. As shown in Fig. 1, we exposed HUVECs to 9 cycles of 1 h hypoxia (0.9% O_2) followed by 36 min of reoxygenation (21% O_2). HUVECs were also exposed to prolonged or cyclic hypoxia for comparable times either with continuous hypoxia (prolonged) or cycles of hypoxia and reoxygenation (cyclic hypoxia). Notably, our previous studies in HUVECs under prolonged hypoxia identified the presence of a switch between the expression of hypoxia inducible factors HIF-1 and HIF-2 that is crucial for the endothelial cell (EC) adaptation to hypoxia and the changes in gene expression that occurred between the two HIFs [15]. Here, we restricted our NGS analyses to 3 main HIF switch transcriptional stages in prolonged hypoxia (0.9% O_2) [15]: (i) an initial stage of hypoxia governed by HIF-1 (prolonged hypoxia for 3 h 12 min compared to 2 cycles of hypoxia/reoxygenation for the same total period of time); (ii) an intermediate stage governed by both HIF-1 and HIF-2 (8 h of prolonged hypoxia compared to 5 cycles of hypoxia/reoxygenation); (iii) and a prolonged stage governed by HIF-2 (14 h and 24 min of prolonged hypoxia compared to 9 cycles of hypoxia/reoxygenation). Both the prolonged and cyclic hypoxia experiments were performed in parallel from the same batch of primary HUVECs cells that were pooled from 10 independent donors and the results were compared to normoxic controls. Since our goal was to determine the specific effects of cyclic hypoxia without the complicating effects of hypoxia, the cyclic hypoxia samples were collected after the full cycle, at the end of the 36 min reoxygenation step.

In HUVECs exposed to cyclic hypoxia for the 3 stages of hypoxia, 72 miRs were significantly changed. 24 miRs were induced and 48 were reduced (Table 1), whereas prolonged hypoxia significantly changed the expression of 121 miRNAs (45 miRs were induced and 76 were reduced) (Fig. 2a; Supplemental Table 1). Notably, the miRNA expression profiles of prolonged and cyclic hypoxia were significantly different and only 4 (including miR-210) and 27 miRs were induced or reduced, respectively, in both models. As shown in Fig. 2b, both models of hypoxia resulted in significant reduction in global miRNA expression. This observation is in agreement with previous reports showing that hypoxia interferes with miRNA biogenesis [18]. Notably, besides the significant differences in miRNA profiles between cyclic and prolonged hypoxia, the global miRNA levels during cyclic hypoxia were less reduced than during prolonged hypoxia (in at each cycle/time tested) (Fig. 2b). Among the miRNAs affected by both hypoxia models, 9 had been previously reported to be hypoxamiRs (Supplemental Table 1) [14,15,19]. The prolonged hypoxia-specific miRNAs included 19 more that were known hypoxamiRs [14,15,19]. Interestingly, none of the miRNAs specifically affected by cyclic hypoxia have been reported before as hypoxamiRs in endothelial cells. These results indicate that cyclic hypoxia affects the miRNA profile in a very different manner than prolonged hypoxia.

When we compared the specific time points with the respective

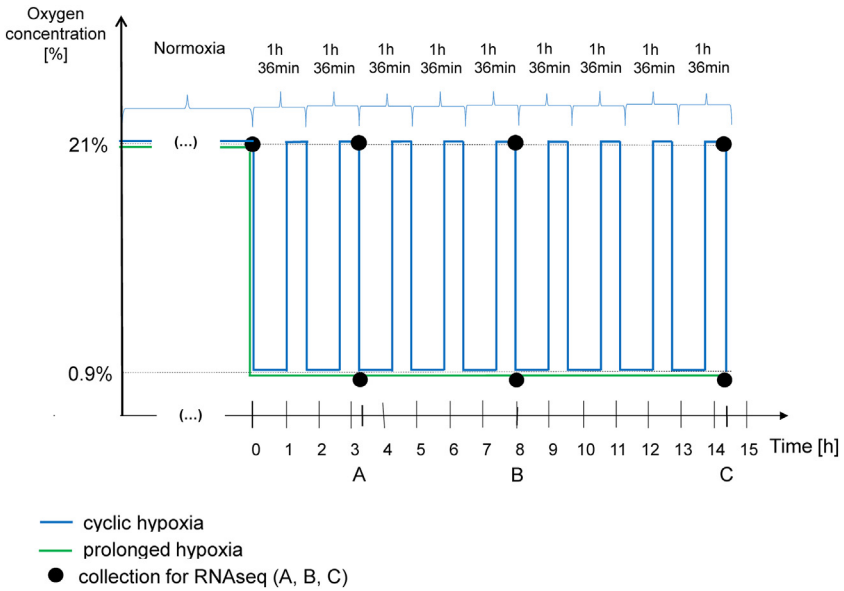

Fig. 1. Schematic representation of cyclic and prolonged hypoxia experiments. HUVECs were placed under cyclic (blue line) and prolonged (green line) hypoxic conditions for the time periods specified. For miRNAseq analysis, samples were isolated at indicated time points (black dots) from cells placed in (i) normoxia, (ii) cyclic and (iii) prolonged hypoxia for 3 h 12 min (A), 8 h (B) and 14 h 24 min (C). (For interpretation of the references to colour in this figure legend, the reader is referred to the web version of this article.)

cycles (Supplementary Fig. 1), both models had very limited impact on miRNAs profiles in the initial stages (after 2 cycles or 3 h of prolonged hypoxia). The levels of only 13 miRs and 20 miRs were affected, respectively, with 5 miRs being common between these two models. During the intermediate stage (after cycle 5 or 8 h of prolonged hypoxia), 33 miRs and 41 miRs were affected, respectively, with 9 miRs in common between the two models. After cycle 9 or 14 h and 24 min of prolonged hypoxia, 37 miRs and 87 miRs were affected (Supplementary Fig. 1), respectively, with 18 miRs in common between these two models. Notably, prolonged cyclic hypoxia affected the miRNA profiles to the lesser extent than the prolonged one.

In order to predict the cyclic hypoxia miRNA effects on the endothelial cell transcriptome, we utilized the miRDIP database. This database effectively combines different target prediction algorithms in order to identify the most probable interactions [45]. Although we limited our analysis to the top 1% of the predicted targets, this identified the highest probability mRNA hits for binding. This analysis identified approximately 6226 of mRNAs being potential targets of miRs affected by cyclic hypoxia and 8674 of potential unique targets for miRs affected by prolonged hypoxia (Supplemental File 1). As shown in Fig. 3, although these models of hypoxia affected a large number of different miRNAs, the majority of potential targets of these miRNAs are common (64.5%; 5842) for cyclic and prolonged hypoxia, whereas the potential exclusive targets in the transcriptome are limited (potential exclusive prolonged targets are 31% (2832)). Interestingly, the exclusive targets for cyclic hypoxia are much more limited (4%; 384). Although these data are based on bioinformatic predictions, they suggest that cyclic and prolonged hypoxia utilize different sets of miRNAs to modulate a number of similar targets of cells signaling (Fig. 3). Moreover, the unique targets of miRNAs that are common between these two types of hypoxia could modulate up to 30% of the targets, but at the same time these targets can be also regulated by miRs unique for either type of hypoxia. The mRNAs that were unique targets for the common miRNA group had no clear GO relation to the cellular response to hypoxia.

Using Gene Ontology Software, we placed these target prediction results into physiological context. As shown in Fig. 3, the common pool of miRNA potential targets for both prolonged and cyclic hypoxia would allow patterns of adaptation to hypoxia that includes cytoskeletal signaling, Wnt/Hedgehog/Notch signaling, MAP kinase signaling, angiogenesis, energy/glucose metabolism and apoptosis and autophagy (Supplemental File 2). Interestingly, the genes that were miRNA target-specific for either prolonged hypoxia or cyclic hypoxia had very limited impact on cell signaling and did not appear to be related to hypoxia.

This data suggest that the cellular adaptation to prolonged and cyclic hypoxia is achieved by differential modulation of expression of a crucial pool of common regulatory genes by distinctive changes in the miRNA modulatory networks. To further test this hypothesis, we followed mRNA changes of genes encoding HIF-1α (*HIF1A)* and HIF-2α (*EPAS1*) (master regulators of hypoxic genes expression), and some downstream effectors including *VEGFA* (main angiogenesis mediator) and *GLUT1* (responsible for adaptation of metabolism to hypoxia). Importantly, both *VEGFA* and *GLUT1* are transcriptionally induced during prolonged hypoxia. As shown in Fig. 4ab, cyclic hypoxia did not result in a dramatic reduction of *HIF1A mRNA* when compared with prolonged hypoxia, and similar to prolonged hypoxia, had a limited effect on *EPAS1* mRNA levels. However, as shown in Fig. 4e, although HIF-1α and HIF-2α accumulate under prolonged hypoxia, the reoxygenation during cyclic hypoxia results in protein degradation. Interestingly, the induced expression of *VEGFA* and *GLUT1* were similar and elevated in both forms of hypoxia (Fig. 4 cd). Notably, the cyclic hypoxia effects on *VEGFA* mRNA levels were less pronounced compared to the prolonged hypoxia. Although these results are limited to two genes, they clearly show the different influence of these hypoxia models on the transcriptional signaling pathways.

In order to verify the usefulness of our functional predictions in the context of anti-angiogenic therapies, we used our NGS data in an *in silico* approach to narrow our focus to the miRNAs uniquely modulated by cyclic hypoxia. These miRNAs display statistically notable and opposite expression profiles during cyclic and prolonged hypoxia, and are dysregulated in various types of cancer and have potential target sites in mRNAs that code for important regulators of hypoxia-induced angiogenesis as predicted by the bioinformatic analysis.

Consequently, we selected miR-19a-5p, an oncomiR that is

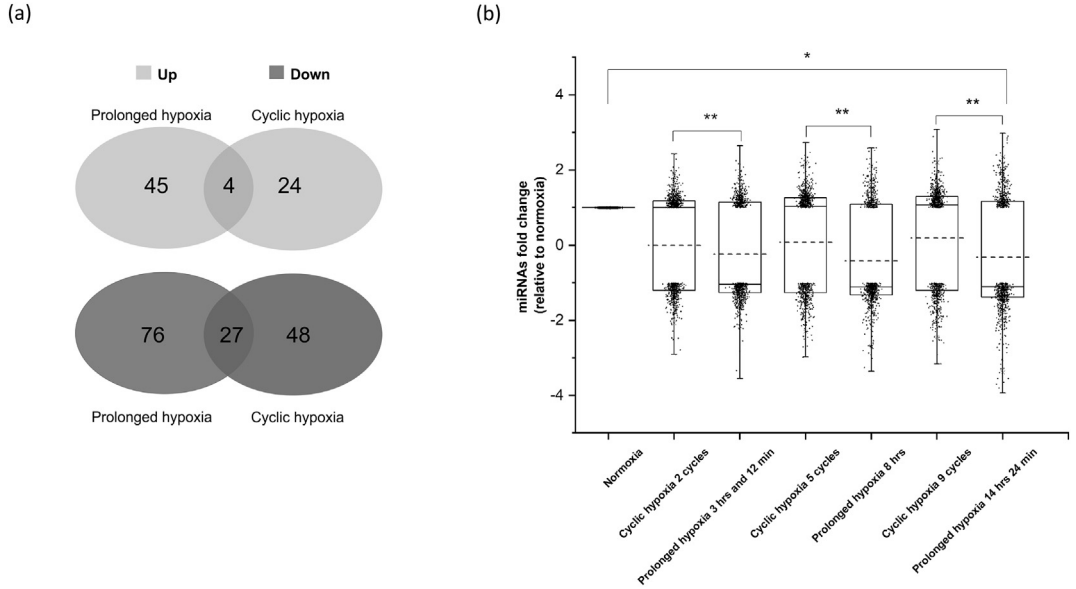

Fig. 2. Cyclic hypoxia has a different effect on the miRNA profiles than prolonged hypoxia. (a) Venn diagrams [44] representing differences in miRNA profiles between the cyclic and prolonged hypoxia models with the numbers of common upregulated and downregulated miRNAs. Light grey denotes upregulation and dark grey denotes downregulation of miRNAs for each condition. (b) Relative miRNAs levels are significantly different during cyclic and prolonged hypoxia when compared to normoxia. The miRNAs levels were expressed as fold change relative to normoxic control, and the groups were compared with ANOVA. *Denote values significantly different between normoxia group and hypoxia groups ($P < .05$). **Furthermore, prolonged hypoxia resulted in more reduced miRNA levels than the cyclic hypoxia (at each cycle/time tested), and the median values are marked with solid lines while average values are dashed.

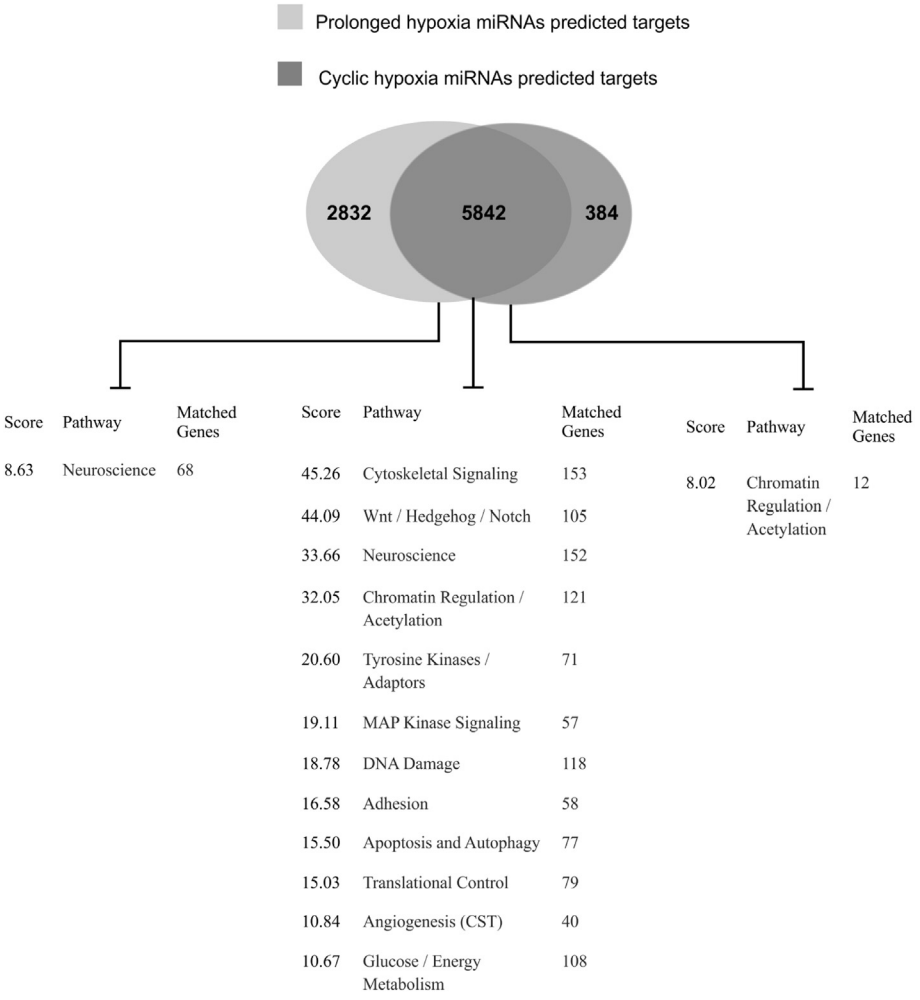

Score	Pathway	Matched Genes
8.63	Neuroscience	68

Score	Pathway	Matched Genes
45.26	Cytoskeletal Signaling	153
44.09	Wnt / Hedgehog / Notch	105
33.66	Neuroscience	152
32.05	Chromatin Regulation / Acetylation	121
20.60	Tyrosine Kinases / Adaptors	71
19.11	MAP Kinase Signaling	57
18.78	DNA Damage	118
16.58	Adhesion	58
15.50	Apoptosis and Autophagy	77
15.03	Translational Control	79
10.84	Angiogenesis (CST)	40
10.67	Glucose / Energy Metabolism	108

Score	Pathway	Matched Genes
8.02	Chromatin Regulation / Acetylation	12

Fig. 3. Venn diagram representing miRDIP's top 1% of predicted targets for miRNAs affected by cyclic and prolonged hypoxia. The signaling pathway targets of miRs affected by the two types of hypoxia are common. The miRNA target roles in cellular signaling and the influence scores were assigned with the GeneAnalytics database. Only high scores (> 10; that represent a significant percentage of matched genes and thus potential involvement in signaling pathways) and medium scores (> 5) were considered.

dysregulated in hepatocellular carcinoma cells under hypoxic conditions [39], in bladder cancer [37] and in lung cancer [38]. As shown in Fig. 5, miR-19a-5p is reduced during cyclic hypoxia, and induced during prolonged hypoxia.

Interestingly, our target prediction analysis identified *HIF1A* and cyclooxygenase-2 (*COX-2),* vascular endothelial growth factor (*VEGF*), vascular endothelial growth factor receptor 1 (*FLT1*), endothelin 1 (*EDN1*), and endothelin-B receptor (*EDNRB*) mRNAs as putative targets of miR-19a-5p. Notably, endothelin signaling has been shown as a critical inducer of cancer angiogenesis [45], while *EDNRB* is predicted to be one of the most probable (top 1% score) targets for miR-19a-5p. Next, using miR-19a-5p analog (mimic) and antagomiR, we tested whether these mRNAs are affected by miR-19a-5p during hypoxia. We looked for mRNAs that are reduced after miR-19a-5p mimic overexpression, and elevated during antagomiR expression. As shown in Fig. 5 and Supplemental Fig. 3, only *EDNRB* mRNA fulfilled these criteria.

The expression of *EDNRB* is elevated during cyclic hypoxia, but not affected by prolonged hypoxia (Fig. 5b). Hence, the downregulation of miR-19a-5p could stimulate angiogenesis through stabilization of *EDNRB* mRNA. Furthermore, overexpression of miR-19a-5p resulted in significant reduction of *EDNRB* mRNA, whereas antagomiR treatment had significant effect on accumulation of this mRNA (Fig. 5c). These results suggest the possibility of a direct interaction between miR-19a-5p and *EDNRB*. This observation, however, would require further analysis to confirm a direct effect. Furthermore, we tested miR-19a-5p effects on mRNA levels of all other predicted mRNA targets that are important for modulation of endothelial response to hypoxia. As shown in Supplemental Fig. 3, miR-19a-5p did not have a direct effect on the majority of these genes. The *HIF1A* and *COX-2* mRNAs levels were unaffected by overexpressed or depleted levels of miR-19a-5p, whereas *EDN1* and *FLT1* mRNAs were reduced by miR-19a-5p mimic only. Notably, a bidirectional influence of miR-19a-5p was observed for *VEGF*, however, the antagomiR effects were minimal.

To test whether miR-19a-5p has a direct effect on blood vessel formation, we performed angiogenic assays in primary HUVECs and overexpressed or depleted miR-19a-5p. As shown in Fig. 6, increasing levels of miR-19a-5p with the specific analog (mimic) impaired tube formation, while depleting HUVECs of physiological levels of miR-19a-5p with an antagomiR had a strong pro-angiogenic effect. This result demonstrates that loss of miR-19a-5p during cyclic hypoxia would be proangiogenic.

It is well known that the endothelial cells show remarkable heterogeneity in structure and function depending on their tissue distribution and other microenvironmental factors [46]. Although HUVECs that are representative for macrovascular endothelium were used as our primary model, we also validated miR-19a-5p's role in primary human dermal microvascular endothelial cells (HMVEC-D). As shown in Fig. 7a, miR-19a-5p is also reduced during cyclic hypoxia in HMVEC-Ds, whereas prolonged hypoxia induces its expression. Furthermore,

Table 1
Cyclic hypoxia-induced changes in miRNAs levels in HUVECs. Cells were exposed to 2, 5 and 9 hypoxic cycles or to the corresponding times of prolonged hypoxia and the miRNA profiles determined with NGS analysis. The detailed fold change values for miRNA affected by either prolonged or cyclic hypoxia are provided in Supplemental Table 1. Only 2 fold changes were considered.

miRNA
Induced during prolonged and cyclic hypoxia
hsa-miR-210-3p (HypoxamiR in ECs and many other types of cells [15,20]); hsa-miR-3974; hsa-miR-4477b; hsa-miR-5095 (HypoxamiR in HUVECs [15]).
Reduced during both prolonged and cyclic hypoxia
hsa-let-7c-3p; hsa-miR-1264; hsa-miR-143-3p (Tumor suppressor in several cancers [21]); hsa-miR-195-3p (Dysregulated in pancreatic cancer [22]); hsa-miR-216b-3p; hsa-miR-26a-1-3p; hsa-miR-301b-5p; hsa-miR-4271; hsa-miR-4472 (HypoxamiR in HUVECs [15]); hsa-miR-4483 (HypoxamiR in HUVECs [15]); hsa-miR-449c-5p (HypoxamiR in HUVECs [15]); hsa-miR-499b-3p (Dysregulated in breast cancer [23]); hsa-miR-520d-5p (Dysregulated in hepatoma [24]); hsa-miR-523-3p; hsa-miR-5581-3p; hsa-miR-5591-5p; hsa-miR-584-3p (Dysregulated in glioma [25]); hsa-miR-586; hsa-miR-599 (HypoxamiR in HUVECs and dysregulated in breast cancer [15,26]); hsa-miR-6083; hsa-miR-6500-5p; hsa-miR-6785-5p (HypoxamiR in HUVECs [15]); hsa-miR-6823-5p; hsa-miR-6865-3p; hsa-miR-6885-5p; hsa-miR-9-3p (Dysregulated in breast cancer [27]); hsa-miR-9-5p (Dysregulated in breast cancer [27]).
Induced during cyclic hypoxia
hsa-miR-191-3p (Dysregulated in hepatocellular carcinoma [28,29]); hsa-miR-3128; hsa-miR-3136-5p; hsa-miR-3193; hsa-miR-3194-5p; hsa-miR-320c (Dysregulated in pancreatic cancer [30]); hsa-miR-3620-3p (Dysregulated in bladder cancer [31]); hsa-miR-3653-3p; hsa-miR-3663-3p (Dysregulated in degenerative aortic stenosis [32]); hsa-miR-3684; hsa-miR-4301 (Dysregulated in colorectal cancer [33]); hsa-miR-450a-5p; hsa-miR-4664-5p; hsa-miR-548u; hsa-miR-641 (Dysregulated in glioblastoma [34]); hsa-miR-6755-3p; hsa-miR-6755-5p; hsa-miR-6817-3p; hsa-miR-744-3p (Dysregulated in pancreatic cancer [35]); hsa-miR-7641
Reduced during cyclic hypoxia
hsa-miR-1257; hsa-miR-1284 (Dysregulated in osteosarcoma [36]); hsa-miR-19a-5p (Dysregulated in bladder cancer [37], lung cancer [38] and hepatocellular carcinoma [39]); hsa-miR-2117; hsa-miR-212-5p; hsa-miR-3120-3p; hsa-miR-3662; hsa-miR-3667-3p (Dysregulated in intracranial aneurysm [40]); hsa-miR-3960 (Dysregulated in type 2 diabetes [41]); hsa-miR-4457; hsa-miR-4650-3p; hsa-miR-4669; hsa-miR-4720-5p; hsa-miR-4778-3p; hsa-miR-4784; hsa-miR-5011-5p; hsa-miR-520 g-5p; hsa-miR-588 (Dysregulated in ovarian cancer [42]); hsa-miR-598-5p (Dysregulated in bile duct cancer [43]); hsa-miR-6770-3p; hsa-miR-7974

depleting these cells of physiological levels of miR-19a-5p with an antagomiR had a strong pro-angiogenic effect (Fig. 7b). Notably, miR-19a-5p analog and antagomiR were able to bidirectional modulate *EDNRB* mRNA levels (Fig. 7c), just as was seen in HUVECs.

3. Discussion

Although cyclic hypoxia has been proposed as a crucial therapeutic target for anticancer therapy, previous studies have focused mainly on prolonged hypoxia models [47,48]. Furthermore, most of the studies conducted so far have focused on the hypoxic microenvironment in tumor cells, while neglecting to follow the consequences of cyclic hypoxia for tumor blood vessel formation [13]. Furthermore, endothelial cells under cyclic hypoxic conditions have been shown to exhibit higher resistance to radiation, greater migration potential and greater tube formation ability [8]. Both cancer and endothelial tissues display different whole genome expression profiles under cyclic and prolonged hypoxia [3]. This difference suggests that the identification of the transcriptional and posttranscriptional factors specific for the cellular adaptation to the cyclic hypoxia may provide novel therapeutic strategies for cancer. The fact that specific miRNAs have been shown to be crucial posttranscriptional mediators for cellular adaptation to prolonged hypoxia suggests that other miRNAs may promote adaptation to cyclic hypoxia [13]. Cyclic hypoxia's influence on endothelial miRNA networks, however, remains unknown. Recently Liu and coworkers identified a cyclic hypoxia-specific interaction between miR-218 and HIF-1α in mouse aortic endothelial cells [49]. To test the hypothesis that cellular adaptation to cyclic hypoxia relies on miRNAs, we have compared miRNA profiles of primary normal endothelial cells exposed to cyclic and prolonged hypoxia. The use of healthy endothelial cells allowed us to identify changes in miRNA levels related to cyclic hypoxia, without the complications associated with the molecular processes triggered by carcinogenesis [3].

As shown in Table 1, cyclic hypoxia has a distinctive effect on HUVEC's miRNA profile, modulating the miRNA network in a very different manner than the prolonged hypoxia. Although, the both hypoxia models have common miRNAs affected (31 miRs: miR-210-3p, miR-3974, miR-4477b, miR-5095, let-7c-3p, miR-1264, miR-143-3p, miR-195-3p, miR-216b-3p, miR-26a-1-3p, miR-301b-5p, miR-4271, miR-4472, miR-4483; miR-449c-5p, miR-499b-3p, miR-520d-5p, miR-523-3p, miR-5581-3p, miR-5591-5p, miR-584-3p, miR-586, miR-599, miR-6083, miR-6500-5p, miR-6785-5p, miR-6823-5p, miR-6865-3p, miR-6885-5p, miR-9-3p, and miR-9-5p.), including miR-210, the majority of miRs induced or reduced by the cyclic hypoxia were different than those identified during prolonged hypoxia. Notably, the large group of miRNAs identified as hypoxamiRs in the prolonged model was reported previously in endothelial cells [15,19]. We collected our prolonged hypoxia data during the time periods that corresponded to the oxygenation/reoxygenation cycles and thus these were different from previous studies [19]. Importantly, none of the miRs that we identified as specific for cyclic hypoxia has been described previously as a hypoxamiR, although the deregulation of many of them has been observed in cancer cells [14,15,19]. Along with the time of exposure of endothelial cells to both hypoxia models, their effect on miRNA levels was more significantly affected at later cycles and during prolonged hypoxia (Supplemental Fig. 1). This is consistent with the previous transcriptomic studies showing that prolonged hypoxia had an extended effect on the transcriptome due to the development of signaling networks and related secondary effects [50,51]. Given that miRNA expression is controlled transcriptionally and often by the HIFs, the observed analysis of miRNA signaling is warranted.

The observed discrepancies in miRNAs profiles between cyclic and prolonged hypoxia suggest that both of these models use miRNAs to modulate different mRNAs in order to adapt the endothelial cells to the low oxygen conditions. In order to verify this hypothesis, we used a bioinformatic approach and found high probability mRNA target genes that could be affected by each hypoxia-specific miRNA network. Interestingly, as shown in Fig. 2, despite the observed differences in miRNA profiles between the prolonged and cyclic hypoxia, their potential target pool was very similar.

To gain a better insight into the functional roles of these putative common and unique cyclic and prolonged hypoxia miRNA targets, these results were placed in a physiological context using a gene ontology approach. The potential targets in common for both hypoxia models were responsible for the cellular adaptation to hypoxia, whereas the potential effects on cellular signaling networks of targets specific for each type of hypoxia were fairly limited. From this analysis, it is clear that the transcriptome's adaptation to cyclic hypoxia is achieved by the different modulation of expression of a set of universal genes for both types of hypoxia that promote angiogenesis, cell survival and a metabolism switch.

The modulation of this gene expression, however, differs between these two types of hypoxia because of the involvement of different miRNA networks that are responsible for destabilizing their mRNA targets. Although adaptation to cyclic hypoxia relies on signaling networks related to the same ones for prolonged hypoxia, their effects are modulated differently by miRNAs. We verified this hypothesis following changes in *HIF1A* and *EPAS1* mRNA levels as well as their transcriptional targets during cyclic and prolonged hypoxia and demonstrated that these models affect HIF mRNA levels differently. Notably, in the current study, we used fast proliferating HUVECs (cultured in the presence of hVEGF, Insulin-Like Growth Factor 1 and hEGF), that were doubling once a day, while we have conducted our

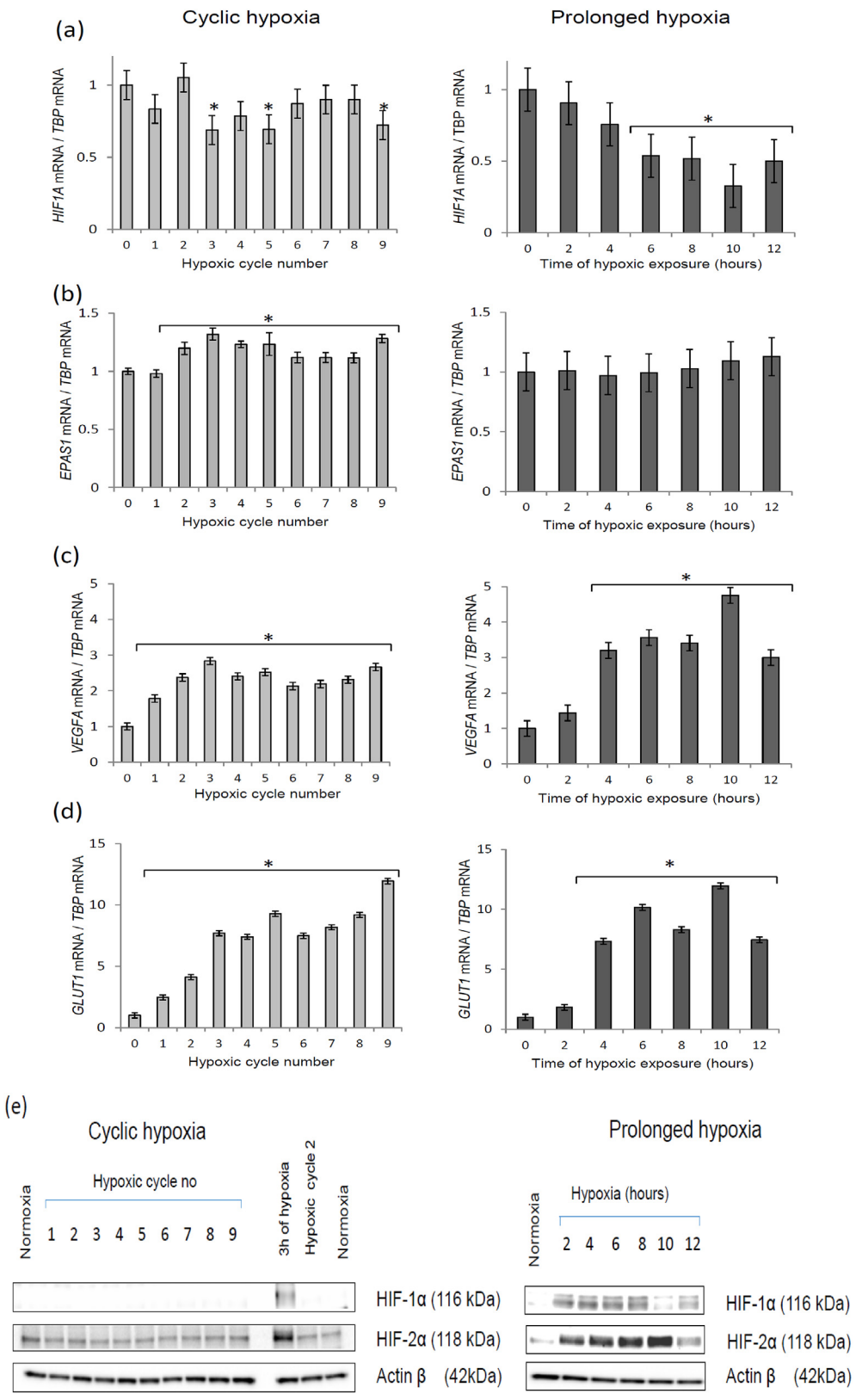

Fig. 4. Cyclic hypoxia (light grey) and prolonged hypoxia (dark grey) have different effects on the expression of the HIF pathway genes. The corresponding mRNA levels of (a) *HIF-1A*, (b) *EPAS1*, (c) *VEGFA* and (d) *GLUT1* from 2 independent experiments ($n = 8$) are plotted normalized to TBP mRNA levels and expressed as a fold-change over the normoxic controls. Error bars represent standard deviations. Significant changes ($P < .05$) are marked with an asterisk. (e) The reoxygenation of HUVECs exposed to cyclic hypoxia results in HIF-1α and HIF-2α protein degradation, while the HIF-1α and HIF-2α accumulate under prolonged hypoxia. The protein lysates were collected after the hypoxic cycle specified (1 h hypoxia and 36 min reoxygenation) and compared with the lysates obtained from cells cultured in normoxia and exposed to 3 h of prolonged hypoxia at the specified times. A representative western blots are shown and β-Actin was used as a loading control.

previous studies using single donor slow proliferating HUVECs (ATTC CRL-1370, a slow growing cell line that has a doubling time of ~5 to 6 days) [52]. Although the hypoxia related changes in HIF-1 protein levels between these two models are correlated, the changes in *HIF1A* mRNA kinetics differ, especially during acute hypoxia, when we do not observe *HIF1A* mRNA accumulation as in ATCC HUVECs. Nevertheless, although the fast proliferating HUVECs are easy to maintain and thus widely used, the turnover of human endothelial cells *in vivo* is over 100 days, whereas the tumor endothelial turn-over can be up to 100 times faster [53]. Although the slow proliferating HUVECs may constitute a more reliable model for following acute hypoxia mRNA changes, the fast proliferating ECs better resemble the tumor

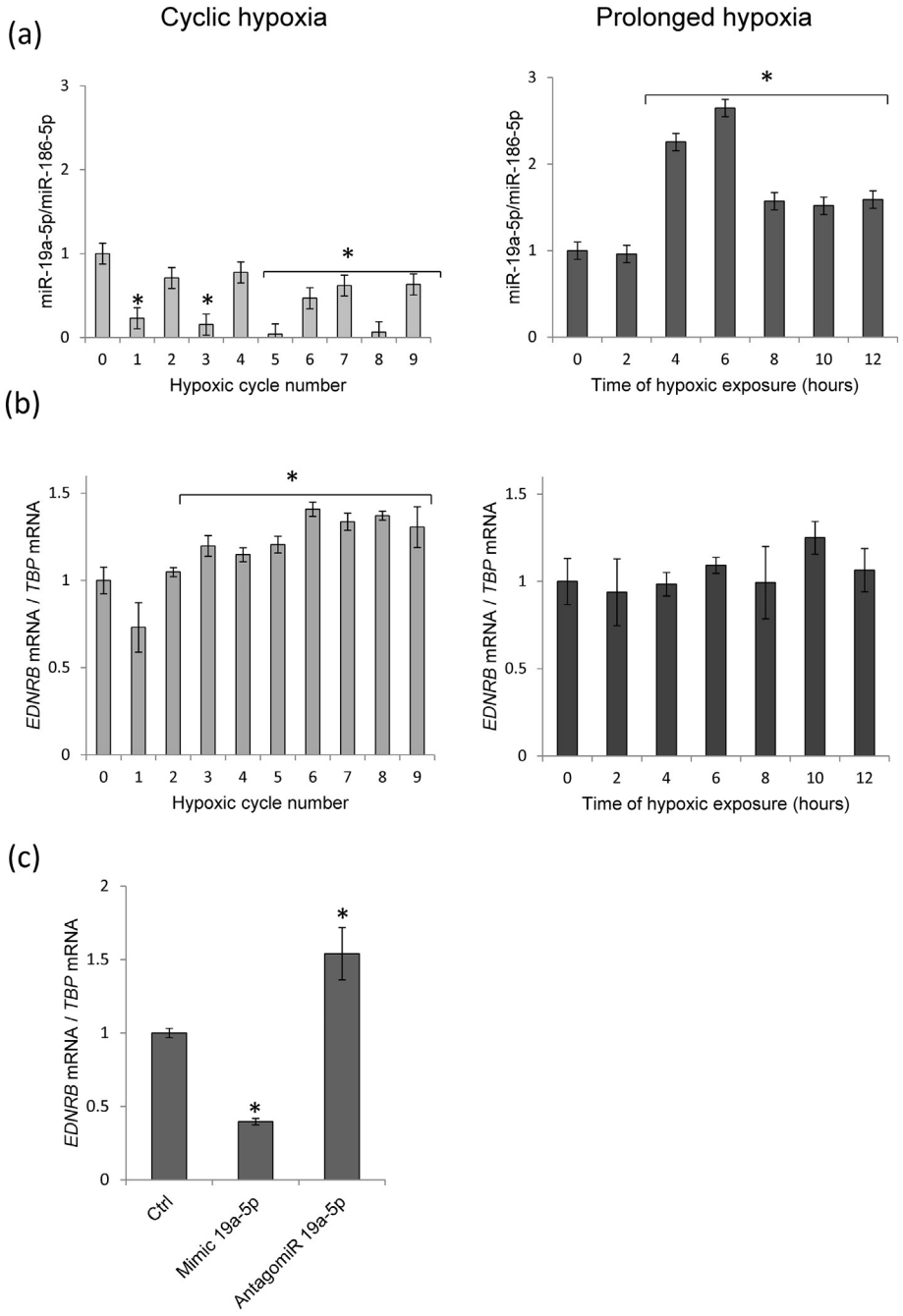

Fig. 5. Cyclic hypoxia (light grey) and prolonged hypoxia (dark grey) have different effects on the expression of miR-19a-5p (a) and its potential target *EDNRB* (b). The corresponding miRNA levels from 2 independent experiments ($n = 8$) are plotted normalized to miR-186-5p levels and expressed as a fold-change over the normoxic controls. The corresponding mRNA levels from 2 independent experiments (n = 8) are plotted normalized to TBP mRNA levels and expressed as a fold-change over the normoxic controls. Error bars represent standard deviations. Significant changes ($P < .05$) are marked with an asterisk. (c) miR-19a-5p regulates *EDNRB* mRNA in primary HUVECs during hypoxia (5 h). The corresponding mRNA levels from 2 independent experiments ($n = 6$) are plotted normalized to TBP levels and expressed as a fold-change over the c67 control.

microenvironment. Since numerous specific miRNAs have been proposed to downregulate *HIF* mRNAs during prolonged hypoxia and none of these miRNAs were identified in this study during cyclic hypoxia, the observed diminished effect on *HIF1A* and *EPAS1* mRNA during cyclic hypoxia supports this hypothesis. Notably, it has been shown that during cyclic hypoxia, HIF-1α is absent during the reoxygenation periods [8,16] (Fig. 4e). Since HIFs were shown to specifically effect miRNAs during prolonged hypoxia, their limited transcriptional impact during cyclic hypoxia could explain differences in the miRNAs profiles. Furthermore, some miRs such as miR-210 [54] were shown to be induced by HIFs during prolonged hypoxia. Our data show that although cyclic hypoxia induces miR-210 expression, this induction is about 5 times lower than in prolonged hypoxia, suggesting that the HIF-related mechanisms of regulating miRNAs levels are limited during the cyclic hypoxia (Supplemental Fig. 2).

Furthermore, our bioinformatic approach suggests that miRNA during both types of hypoxia can be modulators of the chromatin acetylation pathway. Therefore from this group of genes, we selected ones linking HIF transcriptional activity with chromatin acetylation processes that included histone acetyltransferase p300 (*EP300*) *and* CREB-binding protein (*CREBBP*) (co-activators of HIF-1 transcriptional activity) [55], chromobox-like protein 4 (*CBX4*) (enhances HIF-1 activity posttranslationally) [56], *and* exportin-1 (*XPO1*) (mediates miRNA biogenesis and participates in factor inhibiting HIF (*FIH*) export from the nucleus) [57]. As shown in Supplemental Fig. 4, *EP300*, *CREBBP* and *CBX4* mRNAs were induced during prolonged hypoxia and unaffected during cyclic hypoxia. However, the functional consequences of these observations and determining whether miRNAs cause these expression differences will require further studies.

Taken together, our data suggest that endothelial cellular adaptation to cyclic hypoxia is governed by miRNA changes that result in specific modulation of angiogenesis. Hence, this type of miRNA could

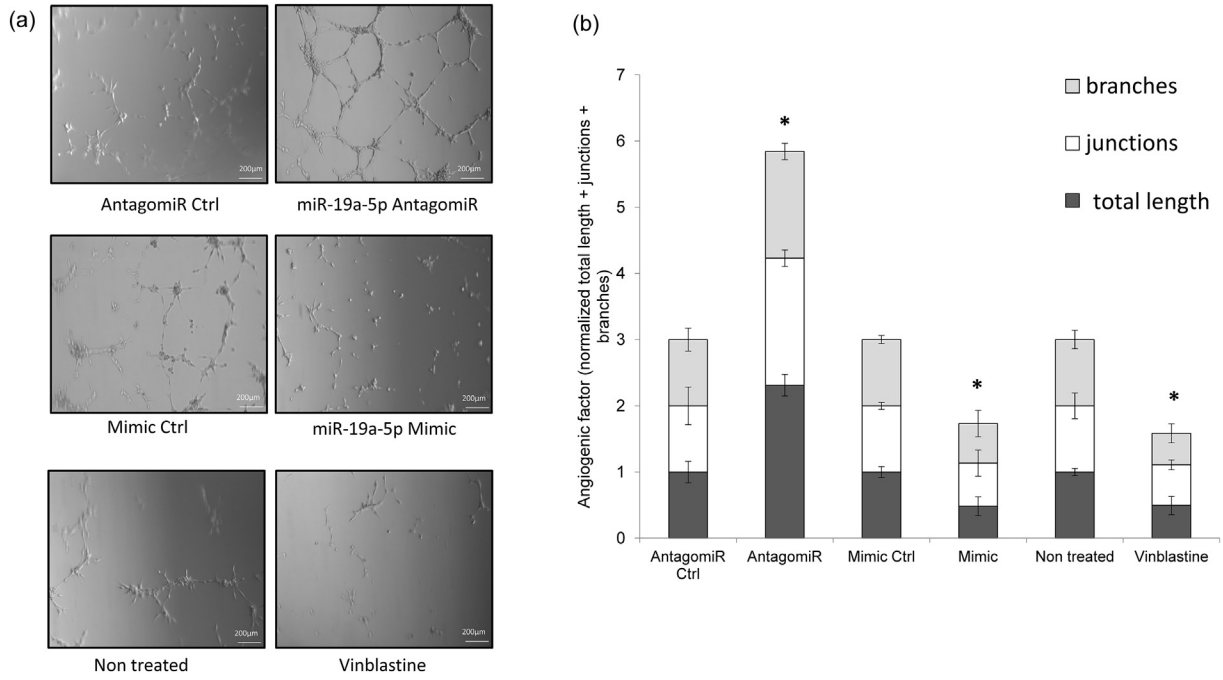

Fig. 6. miR-19a-5p controls angiogenesis in HUVECs. HUVECs were transfected with an antagomiR negative control, miR-19a-5p antagomiR, mimic negative control, miR-19a-5p mimic or treated with vinblastine and cultured for 8 hours in matrigel. Then cells were counted under a microscope at 20 × magnification and their angiogenic factor accessed (total length, the number of created branches and intercellular joints were measured from 6 random focal fields per sample and normalized to the cell number). (a). Representative focal fields illustrating miR-19a-5p's influence on HUVEC morphology in matrigel. (b). The results of the angiogenic factor calculations are plotted normalized to controls and expressed as a fold change over the respectful controls. Error bars represent SD. Significant ($P < 0.05$) changes are marked with an asterisk ("*").

provide a basis for a novel anticancer therapy. In our analysis on miRNAs specific for cyclic hypoxia that were known to be dysregulated in cancer, we identified miR-19a-5p as an efficient modulator of angiogenesis both in macrovascular and microvascular endothelial cells. Furthermore, this miRNA could potentially modulate endothelin-B receptor mRNA, an important mediator of cancer angiogenesis [58]. The effects of overexpression of miR-19a-5p significantly decreased *EDNRB* mRNA levels, illustrating that this miRNA either directly or indirectly strongly influences *EDNRB* mRNA levels.

Moreover, our deep sequencing study identified hypoxamiRs (specific for both cyclic and prolonged hypoxia) that were previously reported as oncomiRs and thus provide a novel link between hypoxia and the cancer microenvironment (Table 1). The oncomiRs include miR-143-3p, miR-195-3p, miR-449b-3p, miR-520d-5p, miR-584-3p, miR-9-3p, miR-9-5p, miR-191-3p, miR-320c, miR-3620-3p, miR-4301, miR-641, miR-744-3p, miR-1284, miR-19a-5p, miR-588, miR-598-5p and miR-210-3p.

In summary, our studies clearly demonstrate that cyclic hypoxia has a very different and specific effect on miRNA profiles of endothelial cells compared to prolonged hypoxia. Interestingly, the physiological changes in the miRNA networks during cyclic hypoxia allows for a specific cellular adaption to this insult through directed modulation of the very same signaling pathways that are responsible for the cellular response to prolonged hypoxia. Furthermore, we show that miRNAs specific for cyclic hypoxia such as miR-19a-5p are potentially important regulators of cellular signaling and thus may provide novel therapeutic strategies for hypoxia and angiogenesis-related diseases.

4. Materials and methods

4.1. Cell lines and culture conditions

Primary HUVECs pooled from 10 independent donors were obtained from Cellworks (division of Catalog Medsystems Ltd., UK). Primary human dermal microvascular cells (HMVEC-D) from a single donor were obtained from Lonza. Both cell lines were maintained until passage five in EGM-2 BulletKit™ medium (Lonza). Cells were split either into 6-well plates or 10 cm dishes and allowed to grow to 70–80% confluence prior to the start of the experiments.

4.2. Induction of hypoxia

Hypoxia was induced in a CO_2/O_2 incubator for hypoxia research (Tri-gas Binder CB150). Briefly, cells were cultured in 35 mm dishes at 0.9% O_2 for the time periods specified. Control cells were maintained in normoxic conditions in the same incubator and harvested at the specified times. Cells maintained in cyclic hypoxia were cultured at 0.9% O_2 for 1 h and then in normoxia for 36 min for the specified number of cycles (1 h 36 min per cycle). The schematic representation of cyclic hypoxia model is depicted in Fig. 1.

4.3. Isolation of RNA and microRNA

Total RNA containing the microRNA fraction was isolated using miRNeasy kit (Qiagen) according to the manufacturer's protocol. RNA concentrations were calculated based on the absorbance at 260 nm. RNA samples were stored at −70 °C until use.

4.4. Next generation RNA sequencing analyses

HUVECs (passage 3) were used for the RNA isolation and analyses. Cells were incubated in normoxia, cyclic hypoxia and prolonged hypoxia conditions for the times specified (Fig. 1) and subsequently used for the RNA isolation and analyses. The induction of hypoxia was verified by accessing miR-210 levels prior to further analysis. MiRNA sequencing libraries were prepared using QIAseq miRNA library kit (Qiagen) following the manufacturer's instructions and followed by sequencing on an Illumina NextSeq instrument. Using Qiagen's

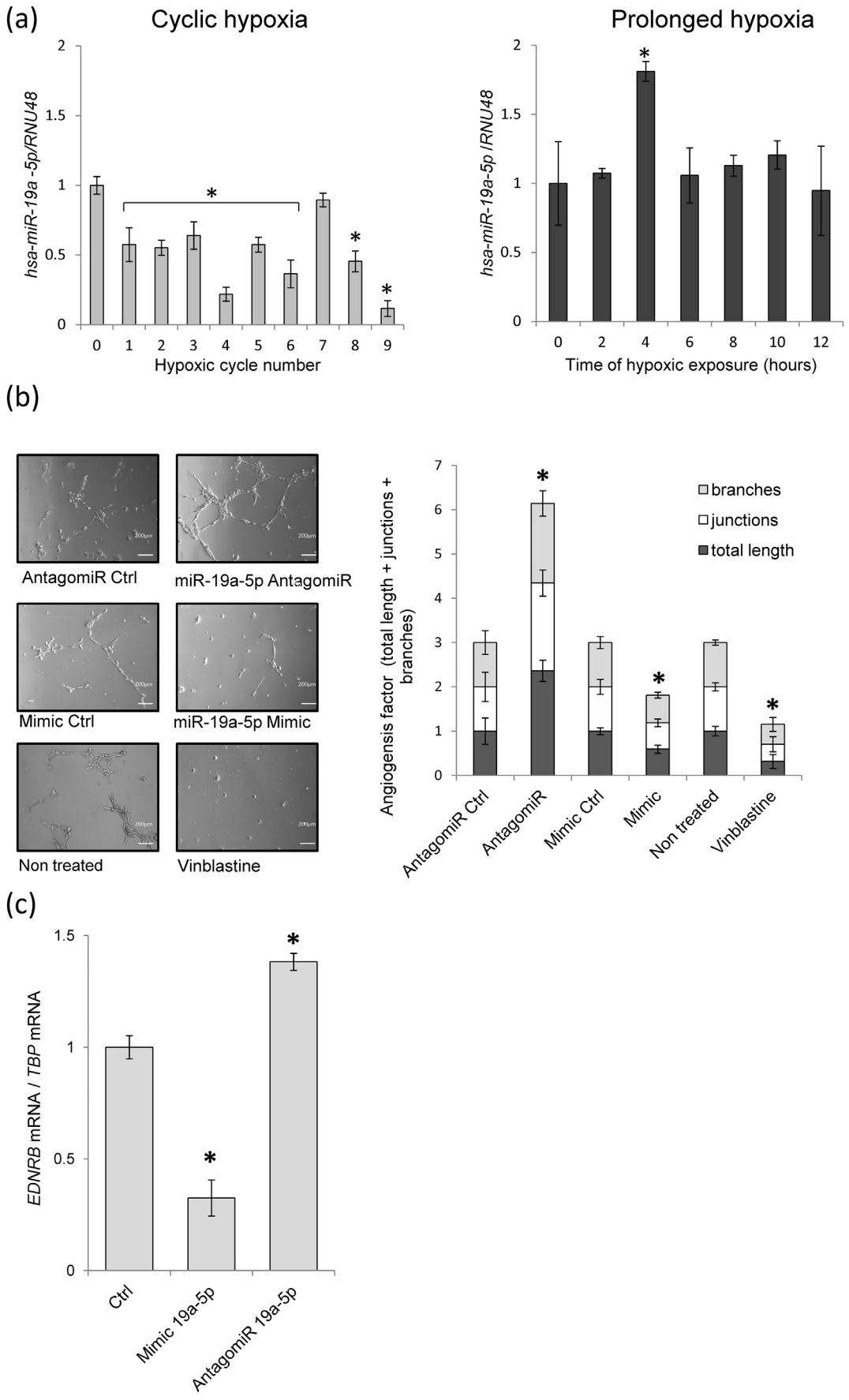

(caption on next page)

Fig. 7. miR-19a-5p controls angiogenesis in HMVEC-Ds. (a) Cyclic hypoxia (light grey) and prolonged hypoxia (dark grey) have different effects on the expression of miR-19a-5p. The corresponding miRNA levels from 2 independent experiments (n = 6) are plotted normalized to *RNU48* levels and expressed as a fold-change over the normoxic controls. Error bars represent standard deviations. Significant changes ($P < 0.05$) are marked with an asterisk. (b). HMVEC-Ds were transfected with an antagomiR negative control, miR-19a-5p antagomiR, mimic negative control, miR-19a-5p mimic or treated with vinblastine and cultured for 8 hours in matrigel. Then cells were counted under a microscope at 20 × magnification and their angiogenic factor accessed (total length, the number of created branches and intercellular joints were measured from 6 random focal fields per sample and normalized to the cell number). Left section - representative focal fields illustrating miR-19a-5p's influence on HMVEC-Ds morphology in matrigel. Right section - the results of the angiogenic factor calculations are plotted normalized to controls and expressed as a fold change over the respectful controls. Error bars represent SD. Significant (p-value < 0.05) changes are marked with an asterisk. (c) miR-19a-5p regulates *EDNRB* mRNA in primary HMVEC-Ds during hypoxia (5 hours). The corresponding mRNA levels from 2 independent experiments (n = 6) are plotted normalized to TBP levels and expressed as a fold-change over the c67 control.

Geneglobe Software, sequencing reads were aligned to the human reference genome assembly (hg19) followed by transcript assembly and estimation of the relative abundances. The analyses of the differential expression of small RNAs between the control (normoxia) and the experimental samples were performed with geNorm (Gene Globe Software) [59]. Next Generation Sequencing experiments were performed by the UAB Heflin Center for Genomic Sciences at UAB. Twofold changes in miRNA levels were considered significant. The resulting data were validated with quantitative real-time PCR. The raw data were deposited in Gene Expression Omnibus (GEO) at accession number GSE116909.

4.5. Bioinformatic analysis of potential miRNA effects

miRNA potential target identification was performed with use of the miRDIP database [45]. The GeneAnalytics™ webserver (geneanalytics.genecards.org) [60] was used to place these targets prediction results in a physiological context and predict potential miRNA effects [61]. The scoring algorithm in the pathways category is based on the algorithm used by the GeneDecks Set Distiller tool [62]. Briefly, all genes in each SuperPath are given a similar weight in the analysis, and the matching score is based on the cumulative binomial distribution. This is used to test the null hypothesis that the queried genes are not over-represented within any SuperPath pathway.

4.6. miRNA analogs and target protector transfections

HUVECs and HMVEC-Ds were transfected in 6-well plates using the liposome Lipofectamine RNAiMAX Transfection Reagent (Thermo Fisher Scientific) according to the manufacturer's protocol. MiR-19a-5p mirVana miRNA Mimic (analog) (assay ID: MC12420) and miR-19a-5p mirVana miRNA antagomiR (assay ID: MH12420) were purchased from Thermo Fisher Scientific and were used at concentrations of 20 and 200 nM, respectively. Cel-miR-67 (Ambion, assay id: MC22484) was used as a negative control. As an additional control for the angiogenic assay-based transfection experiments, Ambion mimic control (no. 4464060) and Ambion antagomiR control (no. 4464076) were used. The transfected cells were cultured for 48 h prior to further analysis.

4.7. Measurement of mRNA and miRNA levels using quantitative real-time PCR

TaqMan RNA-to-CT 1-Step Kit (Thermo Fisher Scientific) was used according to the manufacturer's protocol (relative quantification; Applied Biosystems StepOnePlus Real-Time PCR System). The relative expressions were calculated using the comparative relative standard curve method [63]. *TATA-binding protein* (*TBP*) mRNA was used as the relative control for the studies. We also validated this relative control against rRNA of another housekeeping gene, *18S*. For microRNA real-time PCR experiments, TaqMan Advanced miRNA cDNA Synthesis Kit (Thermo Fisher Scientific) and TaqMan Fast Advanced Master Mix (Thermo Fisher Scientific) were used as described in the manufacturer's protocols. As a relative control for miRNA quantification, we used hsa-miR-186-5p. TaqMan Gene Expression Assay identification (ID) numbers used were: Hs99999901_s1 (*18S*), Hs4332659_m1 (*TBP*), Hs00153153_m1 (*HIF1A*), Hs00900055_m1 (*VEGF*), Hs00892681_m1 (*GLUT1*) Hs00174961_m1 (*EDN1*), Hs00934968_g1 (*EDNRB*), Hs00932878_m1 (*CREBBP*), Hs00185645_m1 (*XPO1*), Hs01106875_g1 (*CBX4*), Hs00914223_m1 (*EP300*), Hs01052961_m1 (*FLT1*), Hs00153133_m1 (*COX-2*).

TaqMan Advanced miRNA Assay identification (ID) numbers were 478750_mir (*hsa-miR-19a-5p*) and 477940_mir (*hsa-miR-186-5p*). TaqMan miRNA Assay identification (ID) numbers were: *hsa-miR-210-3p* (000512); *hsa-miR-19a-5p* (002424*); RNU48* (00106).

4.8. Western blots

Cells were lysed in RIPA buffer (150 mM NaCl, 1% NP-40, 0.5% sodium deoxycholate, 0.1% SDS in 50 mM Tris- HCl, pH 8.0) supplemented with protease Inhibitor Complete Mini (Roche) on ice for 15 min. The cell lysates were rotated at 4 °C for 30 min and the insoluble material was removed by centrifugation at 15,000*g* for 15 min. Protein concentrations were determined by BioRad™ Protein Assay using bovine serum albumin (BSA) as a standard. Following the normalization of protein concentrations, lysates were mixed with an equal volume of 2× Laemmli sample buffer and incubated for 5 min at 95 °C prior to separation by SDS PAGE on stain-free TGX gradient gels (BioRad). Following SDS-PAGE, the proteins were transferred to polyvinylidene fluoride membranes (300 mA for 90 min at 4 °C). The membranes were then blocked with BSA (Sigma-Aldrich) dissolved in TBS/Tween-20 (3% BSA, 0.1% Tween-20 for 1–2 h), followed by immunoblotting with the primary antibody specified for each experiment HIF-1α (Abcam ab16066, diluted at 1:2000); HIF-2α (Abcam ab199, diluted at 1:800), beta Actin (Abcam ab1801, diluted at 1:1000). After the washing steps, the membranes were incubated with goat anti-rabbit IgG (H + L) or with goat anti-mouse IgG (H + L) HRP-conjugated secondary antibodies (BioRad) and detected using ECL (Amresco). Densitometry was performed using Image Lab software v. 4.1 (BioRad).

4.9. Angiogenic assays

Capillary-like structure formations were accessed with the *In Vitro* Angiogenesis Assay Kit (ECM625, Merck Millipore) according to manufacturer's protocol. Briefly, HUVECs or HMVEC-Ds were transfected with miR-19a-5p mirVana miRNA Mimic and miR-19a-5p mirVana miRNA inhibitor (antagomiR) at final concentrations of 20 and 200 nM, respectively. Ambion mimic control and Ambion antagomiR control were used. 48 h after transfection, cells were passaged to matrigel-coated plates. The number of capillary-like structures was counted in each well (from 6 random focal fields at 100× magnification) after 8 h of incubation. A semi-quantitative measurement of capillary structure formation was performed with the Angiosys 2.0 software (Cellworks, Catalog Medsystems Co.; UK). The vinblastine (V1377, Sigma-Aldrich) at a 1 pM final concentration was used as a negative control.

4.10. Statistical analyses

Results were expressed as means ± standard deviations (SD). Statistical significance among means was determined using the Student's *t*-test (two samples, paired and unpaired) or the Kruskal-

Wallis One Way Analysis of Variance on Ranks [64] and Dunn's Method [65] (ANOVA on ranks).

Supplementary data to this article can be found online at https://doi.org/10.1016/j.cellsig.2018.11.020.

Author contributions

Conceived and designed the experiments: R.B. Performed the experiments: K.K., A.M., J.K. All authors analyzed the data. Contributed reagents/materials/analysis tools: K.K. and R.B. Wrote the paper: R.B. and J.F.C. All authors read and revised the final version of the manuscript.

Acknowledgments

This research was funded by National Science Center “Preludium” Program under contract UMO-2015/17/N/NZ7/00962 (K.K.) and a NIHP30 DK072482 and a Research Development Program Grant from the Cystic Fibrosis Foundation (J.F.C.).

Conflicts of interest

The authors declare no conflict of interest. The funders had no role in the design of the study; in the collection, analyses, or interpretation of data; in the writing of the manuscript, and in the decision to publish the results.

References

[1] C. Thirlwell, L. Schulz, H. Dibra, S. Beck, Clin. Epigenetics 3 (9) (2011).
[2] S. Matsumoto, H. Yasui, J.B. Mitchell, M.C. Krishna, Cancer Res. 70 (2010) 10019–10023.
[3] G. Daneau, R. Boidot, P. Martinive, O. Feron, Clin. Cancer Res. 16 (2010) 410–419.
[4] M.W. Dewhirst, Y. Cao, B. Moeller, Nat. Rev. Cancer 8 (2008) 425–437.
[5] P. Martinive, F. Defresne, E. Quaghebeur, G. Daneau, N. Crokart, V. Gregoire, B. Gallez, C. Dessy, O. Feron, FEBS J. 276 (2009) 509–518.
[6] M. Potente, H. Gerhardt, P. Carmeliet, Cell 146 (2011) 873–887.
[7] C. Michiels, C. Tellier, O. Feron, Biochim. Biophys. Acta 1866 (2016) 76–86.
[8] P. Martinive, F. Defresne, C. Bouzin, J. Saliez, F. Lair, V. Gregoire, C. Michiels, C. Dessy, O. Feron, Cancer Res. 66 (2006) 11736–11744.
[9] I. Almendros, D. Gozal, Respir. Physiol. Neurobiol. 256 (2018, October) 79–86.
[10] J.V. Gaustad, T.G. Simonsen, A.M. Roa, E.K. Rofstad, Microvasc. Res. 85 (2013) 10–15.
[11] E.K. Rofstad, J.V. Gaustad, T.A. Egeland, B. Mathiesen, K. Galappathi, Int. J. Cancer 127 (2010) 1535–1546.
[12] J. Nanduri, G. Yuan, G.K. Kumar, G.L. Semenza, N.R. Prabhakar, Respir. Physiol. Neurobiol. 164 (2008) 277–281.
[13] T. Rosenberg, M. Thomassen, S.S. Jensen, M.J. Larsen, K.P. Sørensen, S.K. Hermansen, T.A. Kruse, B.W. Kristensen, CNS Oncol. 4 (2015) 25–35.
[14] P. Madanecki, N. Kapoor, Z. Bebok, R. Ochocka, J.F. Collawn, R. Bartoszewski, Cell. Mol. Biol. Lett. 18 (2013) 47–57.
[15] M. Serocki, S. Bartoszewska, A. Janaszak-Jasiecka, R.J. Ochocka, J.F. Collawn, R. Bartoszewski, Angiogenesis 21 (2018) 183–202.
[16] S. Toffoli, O. Feron, M. Raes, C. Michiels, Biochim. Biophys. Acta 1773 (2007) 1558–1571.
[17] G. Daneau, R. Boidot, P. Martinive, O. Feron, Clin. Cancer Res. 16 (2010) 410–419.
[18] N.R. Gough, Sci. Signal. 6 (2013) ec111-ec111.
[19] A. Janaszak-Jasiecka, A. Siekierzycka, S. Bartoszewska, M. Serocki, L.W. Dobrucki, J.F. Collawn, L. Kalinowski, R. Bartoszewski, Angiogenesis 21 (4) (2018, November) 711–724.
[20] C. Camps, F.M. Buffa, S. Colella, J. Moore, C. Sotiriou, H. Sheldon, A.L. Harris, J.M. Gleadle, J. Ragoussis, Clin. Cancer Res. 14 (2008) 1340–1348.
[21] Z. He, J. Yi, X. Liu, J. Chen, S. Han, L. Jin, L. Chen, H. Song, Mol. Cancer 15 (2016) 51.
[22] B. Zhou, C. Sun, X. Hu, H. Zhan, H. Zou, Y. Feng, F. Qiu, S. Zhang, L. Wu, B. Zhang, Cell. Physiol. Biochem. 44 (2017) 1867–1881.
[23] P. Zou, L. Zhao, H. Xu, P. Chen, A. Gu, N. Liu, P. Zhao, A. Lu, J. Biomed. Res. 26 (2012) 253–259.
[24] S. Tsuno, X. Wang, K. Shomori, J. Hasegawa, N. Miura, Sci. Rep. 4 (2014) 3852.
[25] H. Xue, X. Guo, X. Han, S. Yan, J. Zhang, S. Xu, T. Li, X. Guo, P. Zhang, X. Gao, Q. Liu, G. Li, Oncotarget 7 (2016) 4785–4805.
[26] Y. Wang, Y. Sui, Q. Zhu, X. Sui, Oncol. Lett. 14 (2017) 3455–3462.
[27] R. Barbano, B. Pasculli, M. Rendina, A. Fontana, C. Fusilli, M. Copetti, S. Castellana, V.M. Valori, M. Morritti, P. Graziano, C. Luigi, M. Coco, F. Picardo, T. Mazza, E. Evron, R. Murgo, E. Maiello, M. Esteller, V.M. Fazio, P. Parrella, Sci. Rep. 7 (2017) 45283.
[28] Y. He, Y. Cui, W. Wang, J. Gu, S. Guo, K. Ma, X. Luo, Neoplasia 13 (2011) 841–853.
[29] E. Elyakim, E. Sitbon, A. Faerman, S. Tabak, E. Montia, L. Belanis, A. Dov, E.G. Marcusson, C.F. Bennett, A. Chajut, D. Cohen, N. Yerushalmi, Cancer Res. 70 (2010) 8077–8087.
[30] Y. Iwagami, H. Eguchi, H. Nagano, H. Akita, N. Hama, H. Wada, K. Kawamoto, S. Kobayashi, A. Tomokuni, Y. Tomimaru, M. Mori, Y. Doki, Br. J. Cancer 109 (2013) 502.
[31] K. Popovska-Jankovic, P. Noveski, L. Jankovic-Velickovic, S. Stojnev, R. Cukuranovic, V. Stefanovic, D. Toncheva, R. Staneva, M. Polenakovic, D. Plaseska-Karanfilska, Biomed. Res. Int. 2016 (2016) 7450461.
[32] J. Shi, H. Liu, H. Wang, X. Kong, Biomed. Res. Int. 2016 (2016) 4682172.
[33] A.M. Pehserl, A.L. Ress, S. Stanzer, M. Resel, M. Karbiener, E. Stadelmeyer, V. Stiegelbauer, A. Gerger, C. Mayr, M. Scheideler, G.C. Hutterer, T. Bauernhofer, T. Kiesslich, M. Pichler, Int. J. Mol. Sci. 17 (2016).
[34] D. Paul, A.N. Sinha, A. Ray, M. Lal, S. Nayak, A. Sharma, B. Mehani, D. Mukherjee, S.V. Laddha, A. Suri, C. Sarkar, A. Mukhopadhyay, Sci. Rep. 7 (2017) 2466.
[35] M. Miyamae, S. Komatsu, D. Ichikawa, T. Kawaguchi, S. Hirajima, W. Okajima, T. Ohashi, T. Imamura, H. Konishi, A. Shiozaki, R. Morimura, H. Ikoma, T. Ochiai, K. Okamoto, H. Taniguchi, E. Otsuji, Br. J. Cancer 113 (2015) 1467.
[36] S. Lv, M. Guan, Biosci. Rep. 38 (4) (2018, Jul 13) 1–10, https://doi.org/10.1042/BSR20171675 (BSR20171675).
[37] Y. Feng, J. Liu, Y. Kang, Y. He, B. Liang, P. Yang, Z. Yu, J. Exp. Clin. Cancer Res. 33 (2014) 67.
[38] Y. Gu, S. Liu, X. Zhang, G. Chen, H. Liang, M. Yu, Z. Liao, Y. Zhou, C.-Y. Zhang, T. Wang, C. Wang, J. Zhang, X. Chen, Protein Cell 8 (2017) 455–466.
[39] B. Hu, W.-G. Tang, J. Fan, Y. Xu, H.-X. Sun, Oncol. Lett. 15 (2018) 467–474.
[40] P.X. Li, Q.Y. Zhang, X. Wu, X.J. Yang, Y. Zhang, Y.X. Li, F. Jiang, J. Am. Heart Assoc. 3 (2014).
[41] L. Ding, D. Ai, R. Wu, T. Zhang, L. Jing, J. Lu, L. Zhong, Bioscience, Biotechnol. Biochem. 80 (2016) 461–465.
[42] J. Shen, D. Wang, S.R. Gregory, L. Medico, Q. Hu, L. Yan, K. Odunsi, S.B. Lele, C.B. Ambrosone, S. Liu, H. Zhao, Carcinogenesis 33 (2012) 604–612.
[43] M. Wang, T.-F. Wen, L.-H. He, C. Li, W.-J. Zhu, N.M. Trishul, Int. J. Clin. Exp. Med. 8 (2015) 17261–17270.
[44] H. Heberle, G.V. Meirelles, F.R. da Silva, G.P. Telles, R. Minghim, BMC Bioinform. 16 (2015) 169.
[45] T. Tokar, C. Pastrello, A.E.M. Rossos, M. Abovsky, A.C. Hauschild, M. Tsay, R. Lu, I. Jurisica, Nucleic Acids Res. 46 (2018) D360–D370.
[46] W.C. Aird, Cold Spring Harbor Perspect. Med. 2 (2012) a006429.
[47] B. Muz, P. de la Puente, F. Azab, A.K. Azab, Hypoxia 3 (2015) 83–92.
[48] M. Hockel, P. Vaupel, J. Natl. Cancer Inst. 93 (2001) 266–276.
[49] K.X. Liu, Q. Chen, G.P. Chen, J.C. Huang, J.F. Huang, X.R. He, T. Lin, Q.C. Lin, Oncotarget 8 (2017) 104359–104366.
[50] M.F. Essop, J. Physiol. 584 (2007) 715–726.
[51] M.Y. Koh, G. Powis, Trends Biochem. Sci. 37 (2012) 364–372.
[52] S. Bartoszewska, K. Kochan, A. Piotrowski, W. Kamysz, R.J. Ochocka, J.F. Collawn, R. Bartoszewski, FASEB J. 29 (2015) 1467–1479.
[53] J. Denekamp, Acta Radiol. Oncol. 23 (1984) 217–225.
[54] R.I. McCormick, C. Blick, J. Ragoussis, J. Schoedel, D.R. Mole, A.C. Young, P.J. Selby, R.E. Banks, A.L. Harris, Br. J. Cancer 108 (2013) 1133.
[55] Y. Benita, H. Kikuchi, A.D. Smith, M.Q. Zhang, D.C. Chung, R.J. Xavier, Nucleic Acids Res. 37 (2009) 4587–4602.
[56] J. Li, Y. Xu, X.D. Long, W. Wang, H.K. Jiao, Z. Mei, Q.Q. Yin, L.N. Ma, A.W. Zhou, L.S. Wang, M. Yao, Q. Xia, G.Q. Chen, Cancer Cell 25 (2014) 118–131.
[57] Y. Wang, S. Zhong, C.J. Schofield, P.J. Ratcliffe, X. Lu, J. Cell Sci. (2018) 131.
[58] A. Bagnato, P.G. Natali, J. Transl. Med. 2 (2004) 16.
[59] J. Vandesompele, K. De Preter, F. Pattyn, B. Poppe, N. Van Roy, A. De Paepe, F. Speleman, Genome Biol. 3 (2002) RESEARCH0034.
[60] S. Ben-Ari Fuchs, I. Lieder, G. Stelzer, Y. Mazor, E. Buzhor, S. Kaplan, Y. Bogoch, I. Plaschkes, A. Shitrit, N. Rappaport, A. Kohn, R. Edgar, L. Shenhav, M. Safran, D. Lancet, Y. Guan-Golan, D. Warshawsky, R. Shtrichman, OMICS 20 (2016) 139–151.
[61] R. Bartoszewski, M. Serocki, A. Janaszak-Jasiecka, S. Bartoszewska, K. Kochan-Jamrozy, A. Piotrowski, J. Kroliczewski, J.F. Collawn, Eur. J. Cell Biol. 96 (2017) 758–766.
[62] G. Stelzer, A. Inger, T. Olender, T. Iny-Stein, I. Dalah, A. Harel, M. Safran, D. Lancet, OMICS 13 (2009) 477–487.
[63] A. Larionov, A. Krause, W. Miller, BMC Bioinform. 6 (2005) 62.
[64] W.H. Kruskal, W.A. Wallis, J. Am. Stat. Assoc. 47 (1952) 583–621.
[65] O.J. Dunn, Technometrics 6 (1964) 241.